



Photocatalytic degradation of bagasse pulp wastewater with La-TiO₂/Al₂O₃ as a catalyst

Lihuan Mo^a, Peiqi Lyu^a, Zhen Yang^a, Jie Gong^b, Kai Liu^a, Jun Li^{a,*}

^aSchool of Light Industry and Engineering, South China University of Technology, Guangzhou 510640, China, Tel./Fax: +86 2087110084; emails: ppjunli@scut.edu.cn (J. Li), lhmo@scut.edu.cn (L. Mo), 644201116@qq.com (P. Lyu), 1029974175@qq.com (Z. Yang), 823635902@qq.com (K. Liu)

^bSchool of Environment and Energy, South China University of Technology, Guangzhou 510640, China, email: 245235892@qq.com (J. Gong)

Received 1 August 2019; Accepted 4 January 2020

ABSTRACT

Bagasse pulp wastewater has restricted and disturbed the bagasse pulp industry all the time. In this paper, photocatalytic oxidation technology (O₃+UV+TiO₂) was applied to bagasse pulp wastewater treatment. TiO₂ was prepared into a composite photocatalyst (La-TiO₂/Al₂O₃) to improve the treatment effect. p-Chlorophenol was chosen as a target compound to evaluate the catalytic activity and study the preparation process of La-TiO₂/Al₂O₃. La-TiO₂/Al₂O₃ was finally used in the treatment of real bagasse pulp wastewater with photocatalytic oxidation technology. Under an optimum experiment conditions, chemical oxygen demand (COD) and total organic carbon removal rate of bagasse pulp wastewater reached 80.2% and 77.1%, respectively, and AOX dropped to 2.9 mg/L. Most organic pollutants in the wastewater had been removed. Additionally, in the reusability study, COD removal was maintained at 70.5% at 7th reuse. These findings of present study revealed that La-TiO₂/Al₂O₃ held great potential in the practical photocatalytic degradation application of industrial organic wastewater.

Keywords: Bagasse pulping; Wastewater treatment; TiO₂; Photocatalytic oxidation technology; Composite photocatalyst

1. Introduction

Bagasse, common agricultural waste from sugar industry, is usually used as raw material for pulp and paper industrial. Generally speaking, more than 30 t wastewater needs to be discharged for producing 1 t bleached pulp. Black liquor from pulping section is sent to alkali recovery process, and effluents from pulping washing and screening sections are totally reused. So, the discharge is almost zero in these sections [1]. Actually, the main wastewater which needs to be discharged usually comes from bagasse storage and washing, and the subsequence pulp bleaching [2]. Therefore, pollutants in bagasse pulp wastewater mainly include lignin

fragments and their derivatives, carbohydrate polymers, organic acids, fibers, etc. [3–5]. Its chemical oxygen demand (COD) and biochemical oxygen demand are usually around 1,500 and 1,000 mg/L, respectively. Most of these pollutants are biologically persistent, recalcitrant, and highly toxic to environment [6]. After primary physicochemical treatment and secondary biochemical treatment, the color of wastewater decreases notably. Total organic carbon (TOC), COD, and other contents also have a substantial removal [7]. Still, they could not meet the strict standard [8]. COD of the effluents after secondary treatment is still high (about 200–300 mg/L). Thus, further advanced oxidation process (AOP) is needed to meet the discharge standard [9,10].

* Corresponding author.

AOP, such as Fenton oxidation, ozone oxidation, photocatalytic oxidation, etc., refers to chemical oxidation process involving hydroxyl radicals [9,11–13]. Among them, photocatalytic oxidation has stronger oxidation ability and does not require harsh reaction conditions. As excellent photocatalyst, TiO_2 attracts great attentions, which has advantages of unique optical properties, higher electrical conductivity, longer life span, non-toxic, etc. [14,15]. Photocatalytic oxidation technology ($\text{O}_3+\text{UV}+\text{TiO}_2$) emerged as a promising alternative, which can be applied to advanced treatment of bagasse pulp effluents. Not only can it transfer biologically persistent and recalcitrant pollutants from one phase to another, but also it can degrade those pollutants completely which are difficult to be oxidized by ozone alone. Moreover, with ozone bleaching widely used, the cost of industrial application of ozone is lower than before. The relative low cost of ozone makes it possible that photocatalytic oxidation system ($\text{O}_3+\text{UV}+\text{TiO}_2$) can be successfully put into practice.

However, there are some defects existing in TiO_2 application. TiO_2 has a wide electronic bandgap and hole-electron recombination problem that limited the quantum yield achievable leading to limited photocatalytic properties [16,17]. Thus, it is necessary to narrow down the bandgap of TiO_2 to enhance the utilization of visible light during application process [18]. The doping of rare earth elements can widen the margin of absorption band and improve the separation efficiency of electron hole pairs to get more hydroxyl radicals [19,20]. There are many kinds of dopants, like rare earth metals and alkaline-earth metals. Among these dopants, La-doping modification hinders the phase change (anatase to rutile), which improved the thermal stability and photocatalytic activity [21]. However, the particle of modified TiO_2 remained too small to be recovered [22]. The technology of Al_2O_3 being used in water treatment has already reached mature stage [23,24]. Al_2O_3 , silica-gel, and attapulgite have been used to support TiO_2 preparing catalyst for model and natural water treatment. The TOC removal of the model water (humic acid stock solution) reached 43.3% with $\text{TiO}_2/\text{Al}_2\text{O}_3$, 40.6% with $\text{TiO}_2/\text{silica-gel}$, and 44.0% with $\text{TiO}_2/\text{attapulgite}$ [25,26]. TiO_2 supported on Al_2O_3 is found as the most active catalyst. But single modification can only solve partial problem in application.

In this paper, bagasse pulp wastewater was treated by AOP with photocatalytic oxidation system ($\text{O}_3+\text{UV}+\text{TiO}_2$). To improve the catalytic efficiency and recover rate of TiO_2 , La-doping modification, and Al_2O_3 -loading modification have been combined to prepare the catalyst to make up for the defect of TiO_2 . Hole-electron recombinant problem was ameliorated by La-doping modification, while Al_2O_3 loading modification can make recover and reuse easier. Simulated wastewater (p-chlorophenol as target degradation) was used to study the preparation conditions, because molecular structure of p-chlorophenol is similar to the refractory organic pollutants (chlorinated lignin) in the effluents after secondary biochemical treatment. In order to make the research fit the practical application better, real bagasse pulping effluents after secondary biochemical treatment was used to double-check the activity of catalyst and study the application technology of composite photocatalyst ($\text{La-TiO}_2/\text{Al}_2\text{O}_3$), including application conditions and reusability.

2. Experiment section

2.1. Materials

p-Chlorophenol ($\text{C}_6\text{H}_5\text{OCl}$) for simulative wastewater (300 mg/L solution) preparation was purchased from Aladdin Industrial Corporation, (Shanghai, China). Tetrabutyl titanate [$\text{Ti}(\text{O}-\text{Bu})_4$] was purchased from Chinasun Specialty Products Co., Ltd. (Jiangsu, China). Lanthanum nitrate [$\text{La}(\text{NO}_3)_3 \cdot 6\text{H}_2\text{O}$] was purchased from Sinopharm Chemical Reagent Co., Ltd. (Shanghai, China). Active Al_2O_3 was purchased from Macklin Biochemical Co., Ltd. (Shanghai, China). Anhydrous ethanol and glacial acetic acid was purchased from richjoint Chemical Reagent Co., Ltd. (Shanghai, China).

Pulping wastewater was obtained from secondary sedimentation tank of a bagasse paper mill in Guangxi province. Its basic properties were as follows: $\text{pH} = 7.8 \pm 0.1$, 275 ± 10 Color Unit (C.U.) color, TOC was 65.8 ± 0.5 mg/L, COD was 300 ± 10 mg/L, AOX was 24.6 mg/L.

2.2. Catalyst preparation

Active Al_2O_3 was screened into 40~60, 60~80, and 80~100 mesh. $\text{La-TiO}_2/\text{Al}_2\text{O}_3$ was prepared by ultrasound-assisted sol-gel method.

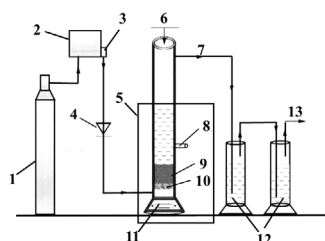
Solution A: 20 mL CH_3OH + 5 mL deionized water + 10 mL CH_3COOH + 0.187 g $\text{La}(\text{NO}_3)_3 \cdot 6\text{H}_2\text{O}$. Solution B: 20 mL $\text{Ti}(\text{O}-\text{Bu})_4$ + 40 mL CH_3OH + 2 mL CH_3COOH . The two solution was stirred continuously with magnetic rotor.

La-TiO_2 sol preparation: all solution A was added into solution B at about 1 drop per second. After the dropping operation was completed, the mixture was kept stirring for 2 h. Then it was treated with an ultrasound generator at 60 Hz (KQ-200VDE Dual frequency numerical control ultrasound instrument, Shumei, China) for 30 min. The prepared mixture was aged at room temperature for 48 h, then the preparation of La-TiO_2 sol was finished.

La-TiO_2 load modification with Al_2O_3 as carrier: the prepared La-TiO_2 sol was divided into three equal parts. Each part was added 6 g active Al_2O_3 with various size. Then the mixture was stirred to make La-TiO_2 sol and Al_2O_3 well mixed. Next, mixture was treated by ultrasound at 60 Hz for a certain time (ultrasound time, one of variables, 0, 5, 10, 15, 20, 25, and 30 min), which could assist La-TiO_2 load on the surface or in internal channels of Al_2O_3 . Mixture was aged at 60°C for 6 h. After calcination at 500°C in muffle furnace for a certain time (calcination time, one of variables, 0.5, 1, 1.5, 2, 2.5, 3, 3.5, 4 h), $\text{La-TiO}_2/\text{Al}_2\text{O}_3$ catalyst was obtained.

2.3. Wastewater treatment and reaction device

The photocatalytic oxidation reaction of the catalyst was completed in the system shown in Fig. 1. The effective volume of the tubular reactor was 500 mL (45 cm high). Oxygen (0.04~0.06 MPa) was piped to ozone generator (Welgo B1-5, Guangzhou) to supply ozone for the system. The mixture of ozone and oxygen was dispersed into the water through the sand chip (16~30 μm). The bagasse pulp wastewater (or simulated wastewater) and catalyst were added to the reactor. The aqueous solution was irradiated with several mercury lamps (every lamp is 15 W), which was set around the reactor to build a UV circumstance. pH value of the



1. oxygen cylinder 2. ozone generator 3. gas flowmeter 4. check valve 5. UV circumstance 6. sampling port 7. outlet 8. sampling port 9. catalyst 10. sand chip 11. reactor 12. KI solution 13. effluent

Fig. 1. Diagram of reaction device.

solution was adjusted by adding NaOH or H_3PO_4 solution. Trail gas was treated by 10 wt.% KI solution.

2.4. Characterizations

XRD patterns of the photocatalyst were recorded using a D8 Advance X-ray diffractometer (Bruker, Germany) with CuK_{α} radiation, operated at 40 kV and 40 mA. The scan rate was $3^{\circ}/min$, with the range of 5° – 90° .

The morphology of catalyst was analyzed by scanning electron microscope (SEM; EVO 18 scanning electron microscope, Zeiss, Germany) at an accelerated voltage of 5 kV. Before SEM observation, catalyst powder should be pasted on the sample plate.

The contents of different elements in catalyst were measured by XRF (Axios X-Ray fluorescence spectrometer, Panlytical, Holland).

BET surface area and pore volume of catalyst were implied from N_2 adsorption-desorption isotherms at 77 K using Micromeritics ASAP 2000 BET surface area analyzer (Norcross, Georgia, USA). Samples were previously out-gassed overnight to ensure a dry clean surface (413 K, 10^{-4} Pa).

Fourier-transform infrared spectroscopy (FT-IR) was used to examine the change of compounds of effluents (Vector 33, Bruker, Germany). The test conditions and method of sample preparation were as follows: the scanning wavelength was set in the range of $4,000$ – 400 cm^{-1} , separation rate was 0.3 cm^{-1} . Signal-noise ratio was 30,000:1. Water sample was filtered by 0.22 μm hydrophilic filter membrane and freeze-dried to obtain the solid powder to make KBr pressing tablet.

TOC of aqueous solution was determined according to ISO 8245 (Multi N/C 3100 total organic carbon and nitrogen analyzer, Analytik Jena, Germany).

AOX was determined by Multi X 2500 total organic halogen analyzer (Analytik Jena, Germany). Treated pulp wastewater sample was diluted 500 times, then filtered by 0.22 μm hydrophilic filter membrane.

COD was determined according to GB 11914-89 (DR6000 multi-parameter water quality analyzer HATCH, USA). Before testing, a standard curve should be plotted by measuring spectrophotometer absorbance for each standard concentration of potassium acid phthalate solution in 25, 50/L, 100, 150, 200, and 250 mg/L. Then COD of the treated effluents were measured.

$$\text{COD removal, \%} = \frac{\text{COD}_{\text{initial}} - \text{COD}_{\text{final}}}{\text{COD}_{\text{initial}}} \times 100$$

3. Results and discussion

3.1. Catalyst preparation

The effects of preparation conditions of $La-TiO_2/Al_2O_3$ on COD removal of simulated wastewater were investigated.

Fig. 2 shows basically positive correlation between COD removal of simulated wastewater and preparation conditions, which included ultrasound loading time, particle size of Al_2O_3 and calcination time. Considering the practical application, the optimized preparation conditions were as follows: ultrasound load time was 20 min, calcination time was 2.5 h, Al_2O_3 particle size was 60–80 mesh.

Ultrasound treatment could promote the loading of $La-TiO_2$ on Al_2O_3 . The relationship between ultrasound loading time and catalytic efficiency was studied. Catalytic efficiency was illustrated by relationship between variable and COD removal. In Fig. 2a, when the ultrasound loading time was 20 min, the catalytic efficiency was highest (COD removal reached 76.9%). During loading process, with the help of ultrasound, $La-TiO_2$ sol-gel would mix with Al_2O_3 uniformly and warp Al_2O_3 particles tightly. Ultrasound provided $La-TiO_2$ energy to load on the surface and enter the internal channels of Al_2O_3 .

Calcination could improve the activity of catalyst. As shown in Fig. 2b, compared with the uncalcined catalyst, the COD removal of calcination with 2.5 h increased by 41.9%. This was because impurities contained in composite photocatalyst would lead to incomplete expose of active sites of catalyst, which would limit the catalytic efficiency of $La-TiO_2/Al_2O_3$ [27]. Calcination process could remove the impurities. But short calcination time could not remove the impurities completely, at the same time there were not enough time to make whole $La-TiO_2$ sol crystallize into $La-TiO_2$ crystal. After sufficiently calcining, $La-TiO_2$ sol was crystallized completely, and the amount of active sites of catalyst was increased by impurities removing. Hence, calcination helped catalyst get good photocatalytic oxidation performance.

The carrier size also had influenced on the load amount of $La-TiO_2$. The COD removal increased with the particle size of Al_2O_3 decreasing (Fig. 2c). This was because the relative load amount of $La-TiO_2$ increased with the decrease of carrier size, and specific surface area and active sites of $La-TiO_2/Al_2O_3$ increased.

3.2. Catalyst load status

Following our previous statement, the composite photocatalyst under optimum preparation conditions was chosen for wastewater treatment. But firstly, it is necessary to illustrate the load status.

Load amount of $La-TiO_2$ and catalytic performance of composite photocatalyst were directly related. In Fig. 3b, Three typical diffraction peaks at $2\theta = 25.3^{\circ}$, 37.8° , and 53.9° corresponding to anatase crystal TiO_2 were observed [28–30]. The content of Ti was 5.06 wt.% in composite catalyst (Fig. 3a). Thus, it was $La-TiO_2$ rather than other titanium compounds that was loaded on Al_2O_3 successfully. There was 0.095 g $La-TiO_2$ loaded on 1 g Al_2O_3 .

From Fig. 3d, it could be seen that the surface of Al_2O_3 was relatively smooth and the pore structure was obvious. However, the surface of $La-TiO_2/Al_2O_3$ was rough and

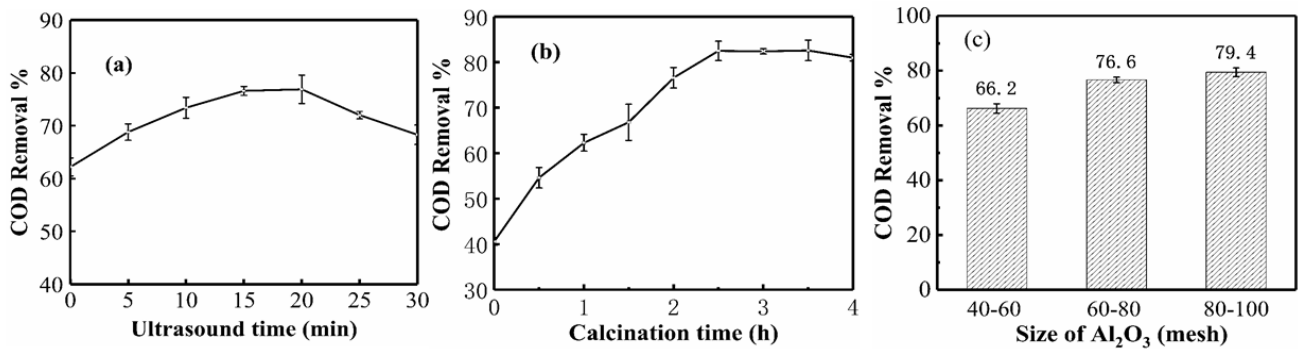


Fig. 2. Study on the preparation conditions of catalyst: (a) The effect of ultrasound load time on the catalyst efficiency, (b) The effect of calcination time on the catalyst efficiency, and (c) The effect of carrier size on the catalyst efficiency. Effluents treatment conditions: the reaction was progressed in the reactor shown in Fig. 1. UV intensity was 45 W (3 mercury lamps around reactor), ozone concentration was 15 mg/L, pH value was 5, catalyst dosage was 10 g/L, and reaction time was 20 min.

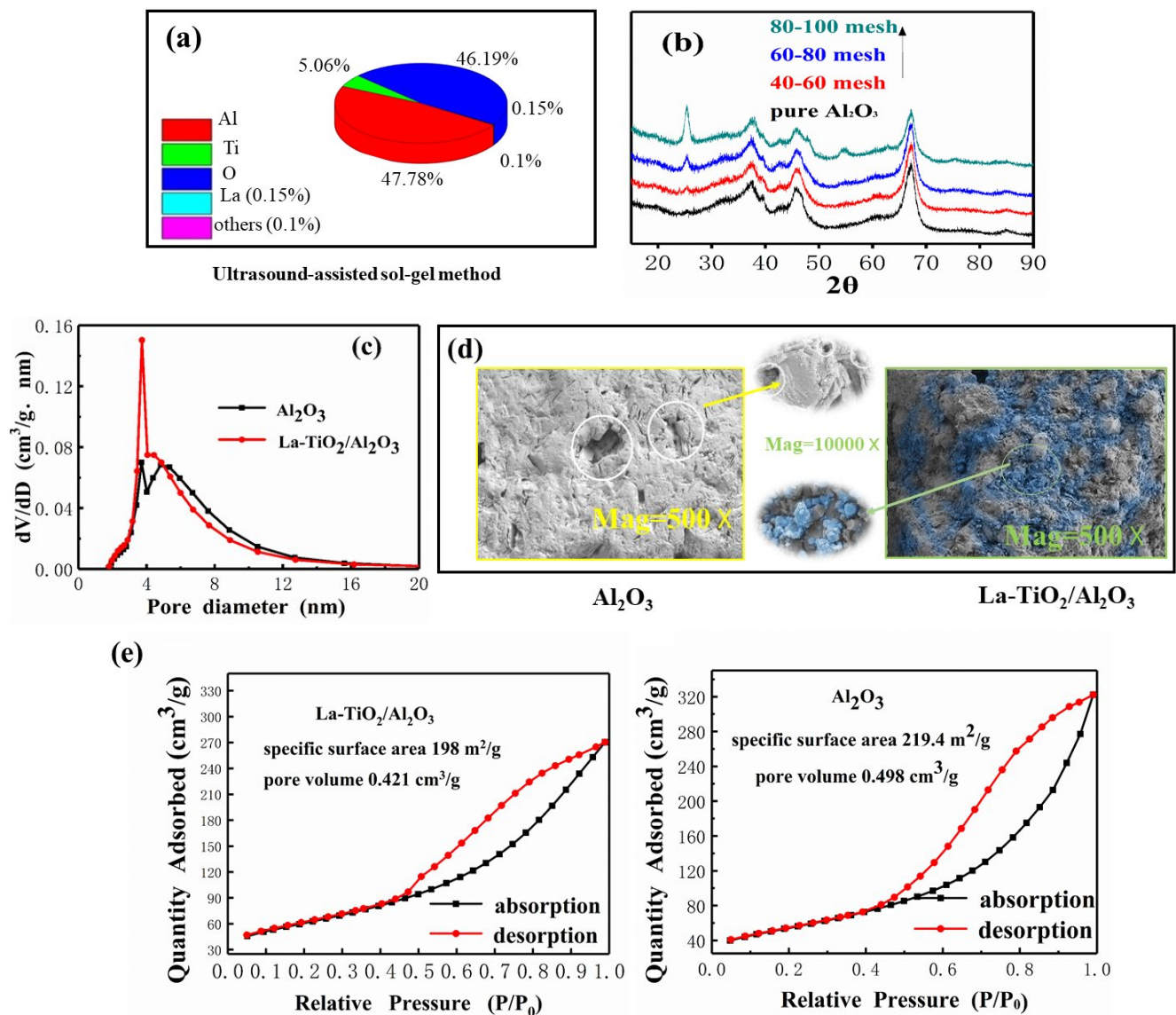


Fig. 3. The characterizations of prepared catalyst: (a) XRF analyses of the La-TiO₂/Al₂O₃ under recommended preparation conditions, (b) XRD patterns of the La-TiO₂/Al₂O₃ with different Al₂O₃ particle size, (c) BJH pore size distribution plots of Al₂O₃ and La-TiO₂/Al₂O₃, (d) SEM image of Al₂O₃ and La-TiO₂/Al₂O₃, and (e) N₂ adsorption/desorption isotherms of Al₂O₃ and La-TiO₂/Al₂O₃.

uneven. It indicated that La-TiO₂ was successfully loaded on the surface of Al₂O₃ [31]. The isotherms corresponding to the Al₂O₃ sample fit in with classical type IV, indicating the Al₂O₃ contained a large amount of mesopores [32,33]. Pore size distribution of Al₂O₃ was mainly concentrated in the range of 3–20 nm, while that of La-TiO₂ was mainly in 8–15 nm (Fig. 3c). So, La-TiO₂ can easily enter the internal channels of Al₂O₃ with the help of ultrasound. The pore volume of La-TiO₂/Al₂O₃ was 0.421 cm³/g, lower than 0.498 cm³/g of Al₂O₃. Compared with Al₂O₃, pore size distribution curve of La-TiO₂/Al₂O₃ moved to the left with average pore size decreasing. The results demonstrated that La-TiO₂ was loaded on both surface and internal channels of Al₂O₃.

3.3. Catalyst efficiency and application

In order to study the effect of photocatalytic oxidation technology (O₃+UV+TiO₂) on bagasse pulp wastewater treatment, pulp wastewater from secondary sedimentation tank of a bagasse pulp mill was used to investigate the factors that affected the wastewater treatment, including reaction time, ozone concentration, UV intensity, and pH value [34–36].

COD reflects the amount of reductive substances pollution and organic pollution in wastewater. TOC indicates the total organic carbon content in wastewater. All

carbon-containing substances, for instance benzene and pyridine, are included in the TOC [37]. Overall, it could be found that COD and TOC variation is very similar in Fig. 4. Both of them showed an obvious upward trend with the increase of ozone concentration, ultraviolet (UV) intensity, and reaction time. Especially with the change of ozone concentration, the curves of COD and TOC removal were basically the same. It suggested that there were almost no reductive substances in real bagasse pulp wastewater from secondary sedimentation tank of a bagasse paper mill. This result was reasonable. Because both COD and TOC removal presented the degradation of lignin fragments and their derivatives in this wastewater. The oxidation of reductive substances and the degradation of carbohydrates mainly occurred in the previous biochemical treatment stage [38]. So, in the following O₃+UV+TiO₂ system, the degradation target of hydroxyl radical [39–43] and ozone was refractory halogenated substances (like chlorinated lignin fragments). With the change of ozone concentration, the value and trend of two dependent variable (COD and TOC removal) were found to be in high level of agreement. Furthermore, the increasing of COD removal rate slowed down with the increasing of variables (reaction time, ozone concentration, UV intensity, and pH value). These trends could help to find the balance between treatment effect and cost of operation. According to the study of application conditions of

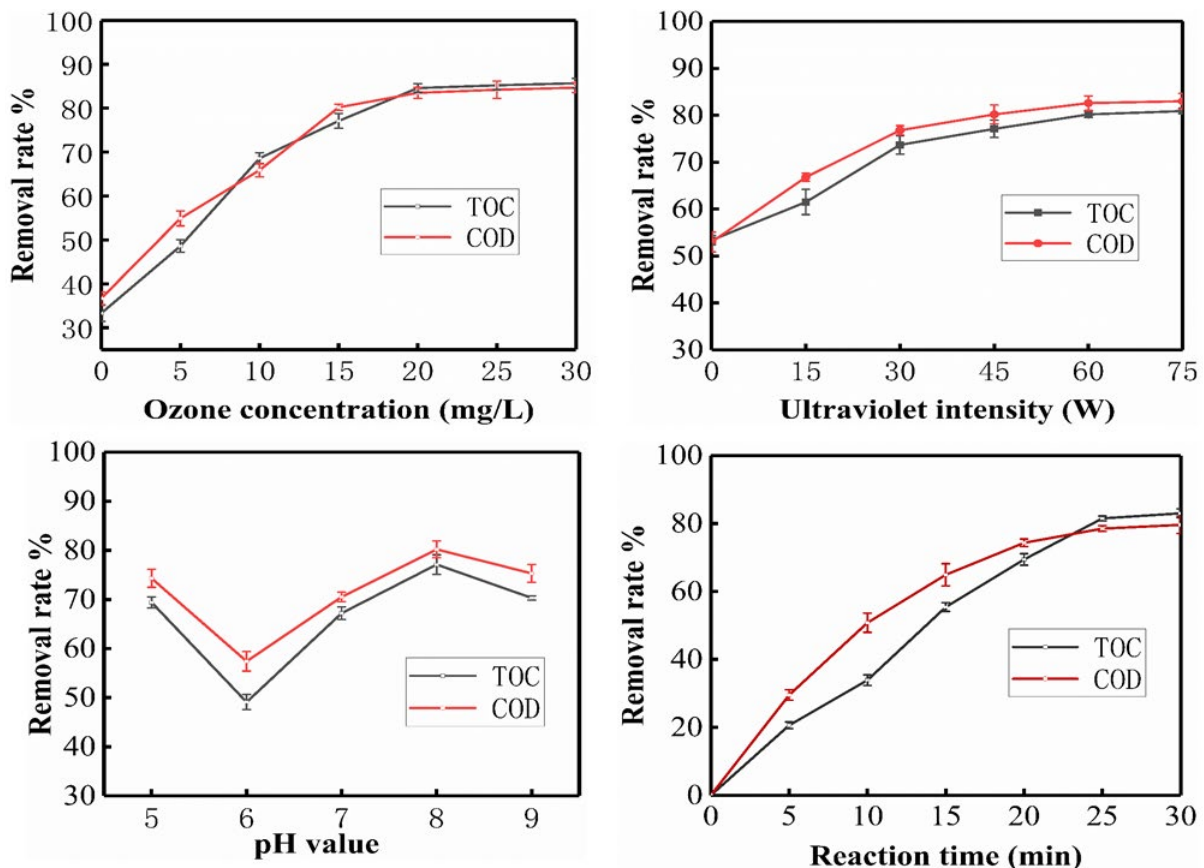


Fig. 4. Exploration of application conditions of the catalyst from aspect of reaction time, UV intensity, ozone concentration, and pH value of the system. The optimum application conditions: reaction time was 25 min, ozone concentration was 15 mg/L, UV intensity was 45 W, pH value was 8.

La-TiO₂/Al₂O₃, an optimum treatment condition for real bagasse pulp wastewater are shown in Fig. 4.

Under treatment conditions in Fig. 4, the relationship between the catalyst dosage and COD and TOC removal was studied. Fig. 5 shows the catalytic effect of La-TiO₂/Al₂O₃ and the dosage of catalyst could reflect the catalytic activity [44,45]. Again, two curves had similar trend. When catalyst dosage was increased from 6 to 16 g/L, COD and TOC removal increased first and then decreased. With dosage of 10 g/L, both COD and TOC removal reached the maximum (80.2% and 77.1%, respectively). But when the dosage kept on increasing, the catalyst showed no noticeable increase, even decreased a little. The previous studies have also reported the similar results [46,47]. This might come as a result of the shielding effect. Excessive catalyst might shield UV light, which affected the function of UV light.

In our study, COD and TOC removal reached 80.2% and 77.1%, respectively. Nano-TiO₂ colloid was employed

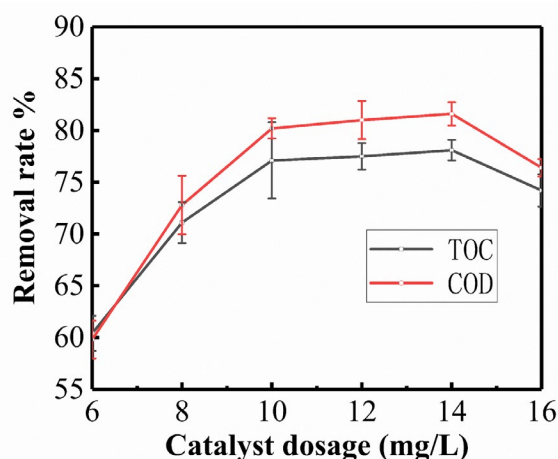


Fig. 5. Effect of catalyst dosage on COD removal rate.

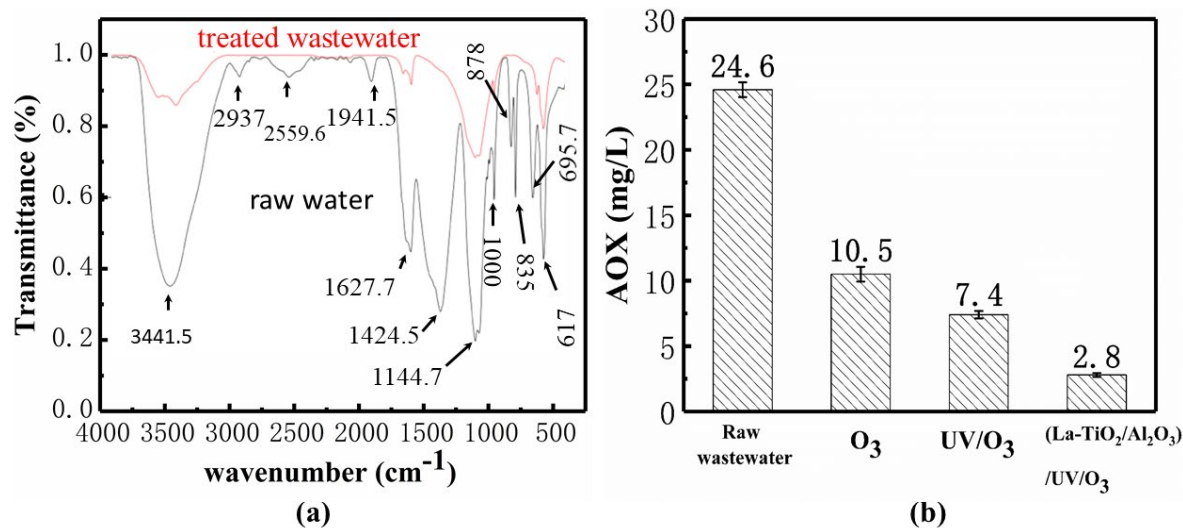


Fig. 6. Analysis of effluent under optimal treatment: (a) Infrared spectrum of treated and untreated wastewater and (b) AOX in wastewater with different system.

in similar papermaking wastewater treatment, and the COD removal reached 66.9% (under optimum process) [48]. Compared with unmodified TiO₂, the composite photocatalyst (La-TiO₂/Al₂O₃) had better catalytic performance. It suggested that the modification of TiO₂ could improve the performance of La-TiO₂/Al₂O₃ in pulp wastewater treatment.

According to Fig. 6b, some pollutants degradation in treated wastewater was observed. The vanished groups could be identified [49,50]. The absorption bands at 1627.7 and 1424.5 cm⁻¹ were assigned to benzene ring [51]. Several narrow peaks at 695.7, 835, and 878 cm⁻¹ were ascribed to the out-of-plane bending vibration of Ar-H [52]. There was a peak at 617 cm⁻¹ for C-Cl bending vibration. This result supported that there were lignin fragments and their derivatives existed (like chlorinated lignin fragments) in real bagasse pulp wastewater, and these biologically persistent, recalcitrant, and highly toxic pollutants were degraded by photocatalytic oxidation technology with La-TiO₂/Al₂O₃ as catalyst. Besides, the FT-IR spectrum exhibited the peak at 1,430–1,629 cm⁻¹ range for C=C bending, and peak at 1,706 cm⁻¹ for C=O bending vibrations. The weakening and disappearing of peaks implied most of the aldehydes, ketones, carboxylic acids, and esters in wastewater were decomposed. Some of them were degraded into small saturated hydrocarbons, or escaped from the water system in CO₂ form.

Absorbable organic halogen (AOX) is also an important index to evaluate the quality of effluent. AOX of the effluent under optimum application conditions was analyzed (shown in Fig. 6). In the discharge standard (GB3544–2008), AOX was taken as a compulsory index (8 mg/L emission). Because of the degradation of chlorinated lignin fragments [53], AOX was reduced from 24.6 to 2.9 mg/L, and the removal rate of AOX was 88.2%. In Parilti's work, Fe(III)/TiO₂/solar UV treatment, was employed to treat paper mill effluent, and the removal rate of AOX was 68% [54]. Fe(III) was added into system to increase the generation rate of hydroxyl radicals. It suggested that modification of TiO₂ could also increase efficiency of degradation of chlorinated lignin fragments.

In many previous studies, simulative wastewater was used to test the efficiency of catalysts. The target degradation compound of simulative wastewater was phenol or methyl orange. So, the final AOX of treated simulative wastewater was very low. But the real industrial wastewater was more complex than simulative wastewater. The final AOX of bagasse pulp wastewater was 2.9 mg/L. Although the AOX of bagasse pulp wastewater was not as low as simulative wastewater, the final AOX (2.9 mg/mL) of bagasse pulp wastewater could meet the discharge standard (8 mg/L emission). Therefore, La-TiO₂/Al₂O₃ showed desirable catalytic effect in treatment of bagasse pulp wastewater with photocatalytic oxidation technology. Not only COD and TOC removal but also AOX has met the standard requirement.

3.4. Stability of catalyst

When evaluating the quality and efficiency of catalyst in industrial applications, the stability, and life cycle of the catalyst were also very important [55,56]. Because the real bagasse pulp wastewater was more complex than simulative wastewater [57], which deactivates the catalyst more quickly. Calcination could combust the organic impurities and increase the catalytic performance. Naturally, when the catalyst reuse was taken into consideration, two methods that was direct reuse and calcination reuse were discussed. Calcination reuse referred to catalyst calcining at 500°C for 1 h then put into next wastewater treatment. In direct reuse, catalyst without additional treat was directly used for next wastewater treatment. The result is shown in Fig. 7. The deactivation of catalyst with direct reuse was faster than calcination reuse. Its COD removal was 83.5% at the first use, and rapidly decreased to 43.4% in the 4th reuse. The catalyst was basically ineffective in the 8th reuse. Because the pollutants in the wastewater would clog the pore channels of the catalyst, and the active sites of catalyst would be covered, then leading to the gradually decrease of the catalyst activity. However, catalytic activity in calcination reuse was relatively stable. In the 4th reuse, the COD removal was kept at 79.8%, just 3.7% lower than the first use. COD removal was maintained at 70.5% in 7th reuse. Organic pollutants adsorbed on catalyst was combusted during

calcination process. Hence, internal channels were dredged and the active sites were exposed again, which made the calcination reuse more stable.

As indicated by Fig. 7, the catalyst with two reuse methods both showed reusability. But, calcination reuse showed better effect than direct reuse. The mesoporous structure of the carrier Al₂O₃ played an important role in the catalytic efficiency [58]. It can increase the amount of catalyst active sites, protect La-TiO₂ from seeping away, and adsorb pollutants to some extent. Therefore, whether the mesoporous structure of the catalyst was well preserved during reuse process was the key factor that affected catalytic efficiency and reusability. As shown in Fig. 8a, both calcination and direct reused catalyst still have mesoporous structure [59]. However, compared with direct reuse, calcination reused catalyst were closer to the unused catalyst. Consistent with the specific surface area and pore volume of catalyst, direct reused got lower dates—188.6 m²/g and 0.393 cm³/g. Unused catalyst was 198.0 m²/g and 0.421 cm³/g, while calcination reuse was 197.2 m²/g and 0.413 cm³/g. Thus, calcination was more appropriate for catalyst reusing.

Even though effects of calcination reuse were stable, the trend of calcination reuse curve was still downward. It could be observed in Fig. 8b that mesoporous structure of catalyst with 4th calcination reuse became large and increased in number. The reason was that repeated calcination led some internal channels collapse and made small holes interoperable into large holes. Fig. 8d showed no change in crystalline of catalyst, which meant crystalline was not the reason for the decrease of catalytic efficiency. In Fig. 8c, the content of Ti decreased gradually with the increase of reuse times. After 6th reuse, the Ti content dropped to 3.02%. If catalyst continued to be used, La-TiO₂ would keep on losing. These results demonstrated that repeated calcination made the channels of catalyst become large and weaken the protection of La-TiO₂. Finally, gradual loss of La-TiO₂ made catalytic performance worse and worse in reuse process [60].

According to our experiment data, preliminary cost of the treatment was 10 RMB/t. It was too expensive for industrial treatment. Our subsequent study would focus on how to cut down the cost.

4. Conclusion

In this paper, the preparation and application of photocatalytic catalyst (La dope modified TiO₂ supported by Al₂O₃) were studied, and real bagasse pulp wastewater was treated by photocatalytic technology (O₃+UV+TiO₂). The preparation conditions for La-TiO₂/Al₂O₃ was optimized (supersonic loading time was 20 min, calcination time was 2.5 h, Al₂O₃ particle size was 60–80 mesh). The obtained catalyst had a mesoporous structure. And there was 0.095 g La-TiO₂ loaded on 1 g Al₂O₃. Based on introducing Al₂O₃ as carrier to load La-TiO₂, the composite photocatalyst had better efficiency on treatment of bagasse wastewater. The COD and TOC removal of bagasse pulp wastewater were 80.2% and 77.1%, respectively, and AOX dropped to 2.9 mg/L. At the same time, the catalyst also had ideal performance in reuse process, and the COD removal was maintained at 70.5% at 7th calcination reuse. Based on the real bagasse wastewater treatment, the results of this paper could provide reference

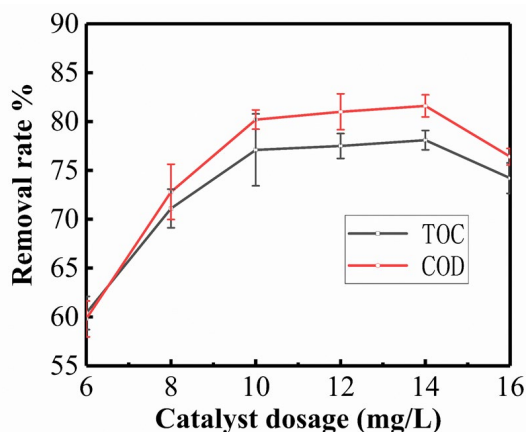


Fig. 7. Reusability of direct reuse and calcination reuse.

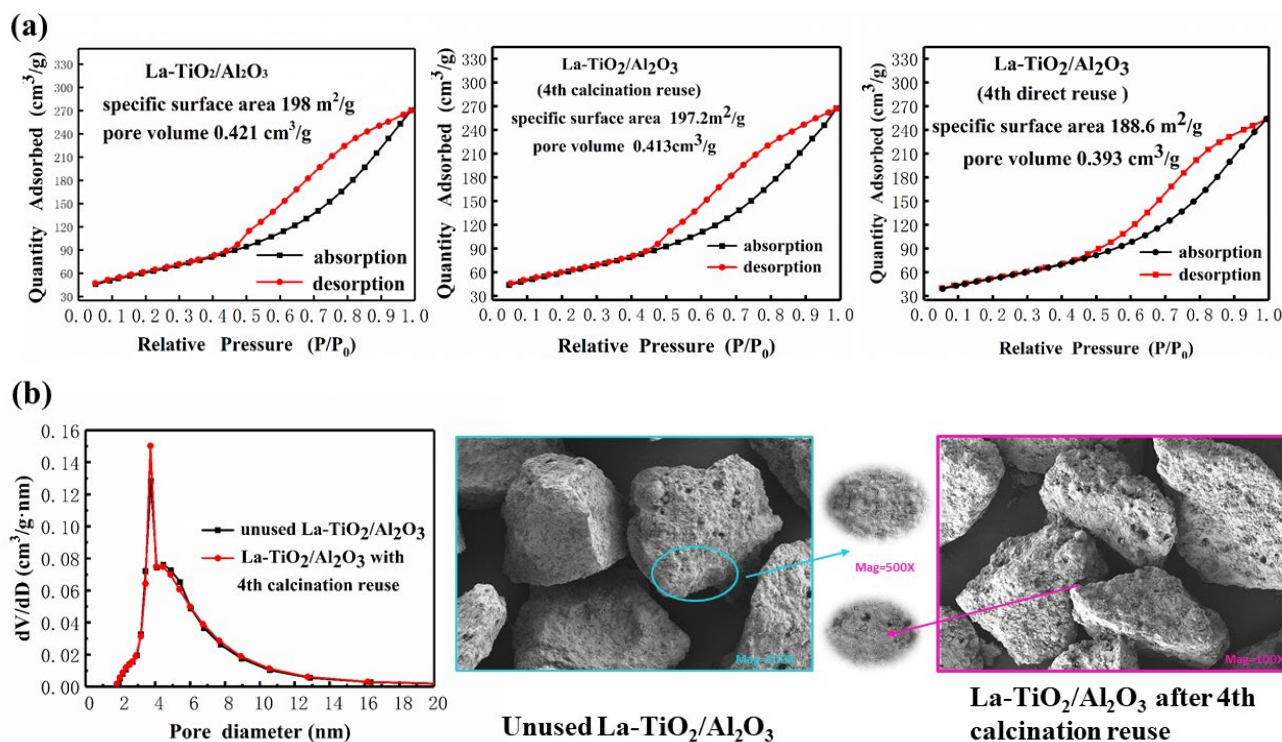


Fig. 8. Characterization of Catalyst before and after reuse: (a) N₂ adsorption/desorption isotherms of catalyst before and after reuse, (b) Pore size distribution plots of catalyst before and after use and SEM image of La-TiO₂/Al₂O₃ with 4th calcination reuse, (c) XRF of La-TiO₂/Al₂O₃ with different calcination reuse times, and (d) XRD patterns of La-TiO₂/Al₂O₃ at 6th calcination reuse.

for the application practice of bagasse pulp wastewater with photocatalytic technology (O₃+UV+TiO₂).

Acknowledgments

The authors gratefully acknowledge the financial support of Guangzhou Science and Technology Plan Projects (201707020011), the Special Support Plan for High-level Talent Cultivation of Guangdong Province (No. 2014TQ01N603), the State Key Laboratory of Pulp and Paper Engineering (201831), and Guangdong Province Science Foundation for Cultivating National Engineering Research Center for Efficient Utilization of Plant Fibers (2017B090903003).

References

- [1] A. Blanco, D. Hermosilla, C. Negro, Wastewater Reuse and Current Challenges: Water Reuse Within the Paper Industry, Springer, Cham, Switzerland, 2015.
- [2] R. Sridhar, V. Sivakumar, K. Thirugnanasambandham, Response surface modeling and optimization of upflow anaerobic sludge blanket reactor process parameters for the treatment of bagasse based pulp and paper industry wastewater, Desal. Water Treat., 57 (2015) 1–12.
- [3] A. Raj, S. Kumar, I. Haq, S.K. Singh, Bioremediation and toxicity reduction in pulp and paper mill effluent by newly isolated ligninolytic *Paenibacillus* sp., Ecol. Eng., 71 (2014) 355–362.
- [4] P.C. Lindholm-Lehto, J.S. Knuutinen, H.S.J. Ahkola, S.H. Herve, Refractory organic pollutants and toxicity in pulp and paper mill wastewaters, Environ. Sci. Pollut. Res., 22 (2015) 6473–6499.
- [5] S.J. Jahren, J.A. Rintala, H. Ødegaard, Aerobic moving bed biofilm reactor treating thermomechanical pulping whitewater under thermophilic conditions, Water. Res., 36 (2002) 1067–1075.
- [6] N. Jaafarzadeh, F. Ghanbari, M. Ahmadi, M. Omidinasab, Efficient integrated processes for pulp and paper wastewater treatment and phytotoxicity reduction: permanganate, electro-Fenton and Co₃O₄/UV/peroxymonosulfate, Chem. Eng. J., 308 (2017) 142–150.
- [7] M.A. Hubbe, J.R. Metts, D. Hermosilla, M.A. Blanco, L. Yerushalmi, F. Haghghat, P. Lindholm-Lehto, Z. Khodaparast, M. Kamali, A. Elliott, Wastewater treatment and reclamation: a review of pulp and paper industry practices and opportunities, BioResources, 11 (2016) 7953–8091.
- [8] C. Zhang, J. Chen, Z. Wen, Alternative policy assessment for water RO pollution control in China's pulp and paper industry, Resour. Conserv. Recycl., 66 (2012) 15–26.
- [9] D. Hermosilla, N. Merayo, A. Gascó, A. Blanco, The application of advanced oxidation technologies to the treatment of effluents from the pulp and paper industry: a review, Environ. Sci. Pollut. Res., 22 (2015) 168–91.
- [10] N. Merayo, D. Hermosilla, L. Blanco, L. Cortijo, Á. Blanco, Assessing the application of advanced oxidation processes, and their combination with biological treatment, to effluents from pulp and paper industry, J. Hazard. Mater., 262 (2013) 420–427.
- [11] N.N. Mahamuni, Y.G. Adewuyi, Advanced oxidation processes (AOPs) involving ultrasound for wastewater treatment: a review with emphasis on cost estimation, Ultrason. Sonochem., 17 (2010) 990–1003.
- [12] X. Lü, Q. Zhang, W. Yang, X. Li, L. Zeng, L. Li, Catalytic ozonation of 2, 4-dichlorophenoxyacetic acid over novel Fe-Ni/AC, RSC Adv., 5 (2015) 10537–10545.
- [13] P. Liu, S. He, H. Wei, J. Wang, C. Sun, Characterization of α -Fe₂O₃/ γ -Al₂O₃ catalysts for catalytic wet peroxide oxidation of m-cresol, Ind. Eng. Chem. Res., 54 (2016) 130–136.
- [14] Y. Zhang, Y. Zhao, S. Cao, Z. Yin, L. Wu, Design and synthesis of hierarchical SiO₂@C/TiO₂ hollow spheres for high performance supercapacitors, ACS Appl. Mater. Interfaces, 9 (2017) 29982–29991.

- [15] X.C. Li, W.J. Zheng, G.H. He, R. Zhao, D. Liu, Morphology control of TiO₂ nanoparticle in microemulsion and its photocatalytic property, *ACS Sustainable Chem. Eng.*, 2 (2013) 288–295.
- [16] C. Adán, A. Bahamonde, M. Fernández-García, A. Martínez-Arias, Structure and activity of nanosized iron-doped anatase TiO₂ catalysts for phenol photocatalytic degradation, *Appl. Catal., B*, 72 (2007) 11–17.
- [17] A. Banisharif, A.A. Khodadadi, Y. Mortazavi, A. Anaraki Firooz, J. Beheshtian, S. Agah, S. Menbari, Highly active Fe₂O₃-doped TiO₂ photocatalyst for degradation of trichloroethylene in air under UV and visible light irradiation: experimental and computational studies, *Appl. Catal., B*, 165 (2015) 209–221.
- [18] G. Matafonova, V. Batoev, Recent advances in application of UV light-emitting diodes for degrading organic pollutants in water through advanced oxidation processes: a review, *Water Res.*, 132 (2018) 177–189.
- [19] L. Song, X. Zhao, L. Cao, J.W. Moon, B. Gu, W. Wang, Synthesis of rare earth doped TiO₂ nanorods as photocatalysts for lignin degradation, *Nanoscale*, 7 (2015) 16695–16703.
- [20] C. Byrne, L. Moran, D. Hermsilla, N. Merayo, Á. Blanco, S. Rhatigan, S. Hinder, P. Ganguly, M. Nolan, S.C. Pillai, Effect of Cu doping on the anatase-to-rutile phase transition in TiO₂ photocatalysts: theory and experiments, *Appl. Catal., B*, 246 (2019) 266–276.
- [21] Y. Zhang, H. Zhang, Y. Xu, Y. Wang, Significant effect of lanthanide doping on the texture and properties of nanocrystalline mesoporous TiO₂, *J. Solid State Chem.*, 177 (2004) 3490–3498.
- [22] Y.H. Chen, M. Franzreb, R.H. Lin, L.L. Chen, P.C. Chiang, Platinum-doped TiO₂/magnetic poly(methyl methacrylate) microspheres as a novel photocatalyst, *Ind. Eng. Chem. Res.*, 48 (2009) 7616–7623.
- [23] M. Trueba, S.P. Trasatti, γ -alumina as a support for catalysts: a review of fundamental aspects, *Eur. J. Inorg. Chem.*, 17 (2005) 3393–3403.
- [24] B. Kasprzyk-Hordern, Chemistry of alumina, reactions in aqueous solution and its application in water treatment, *Adv. Colloid Interface Sci.*, 110 (2004) 19–48.
- [25] R. Gracia, S. Cortés, J. Sarasa, P. Ormad, J.L. Ovelheiro, Heterogeneous catalytic ozonation with supported titanium dioxide in model and natural waters, *Ozone Sci. Eng.*, 22 (2000) 461–471.
- [26] A.G. Thomas, K.L. Syres, Adsorption of organic molecules on rutile TiO₂ and anatase TiO₂ single crystal surfaces, *Chem. Soc. Rev.*, 41 (2012) 4207–4217.
- [27] X.L. Jia, Y. Wang, R.S. Xin, Q.L. Jia, H.J. Zhang, Preparation of rare-earth element doped titanium oxide thin films and photocatalysis properties, *Key Eng. Mater.*, 336–338 (2007) 1946–1948.
- [28] Y. Chen, Q. Wu, N.S. Bu, J. Wang, Y.T. Song, Magnetic recyclable lanthanum-nitrogen co-doped titania/strontium ferrite/diatomite heterojunction composite for enhanced visible-light-driven photocatalytic activity and recyclability, *Chem. Eng. J.*, 373 (2019) 192–202.
- [29] T.G. Deepak, D. Subash, G.S. Anjusree, K.R.N. Pai, S.V. Nair, A.S. Nair, Photovoltaic property of anatase TiO₂ 3-D mesoflowers, *ACS Sustainable Chem. Eng.*, 2 (2014) 2772–2780.
- [30] J. Yoon, E. Shim, S. Bae, H. Joo, Application of immobilized nanotubular TiO₂ electrode for photocatalytic hydrogen evolution: reduction of hexavalent chromium (Cr(VI)) in water, *J. Hazard. Mater.*, 161 (2009) 1069–1074.
- [31] S. He, J. Li, J. Xu, L. Mo, Enhanced removal of COD and color in paper-making wastewater by ozonation catalyzed by Fe supported on activated carbon, *BioResources*, 11 (2016) 8396–8404.
- [32] J.G. Yu, Y.R. Su, B. Cheng, Template-free fabrication and enhanced photocatalytic activity of hierarchical macro-/mesoporous titania, *Adv. Funct. Mater.*, 17 (2007) 1984–1990.
- [33] M.L. Garcia-Benjume, M.I. Espitia-Cabrera, M.E. Contreras-Garcia, Enhanced photocatalytic activity of hierarchical macroporous anatase by ZrO₂ incorporation, *Int. J. Photoenergy*, 2012 (2012) 1–10.
- [34] M. Ahmadi, B. Kakavandi, N. Jaafarzadeh, A. Akbar Babaei, Catalytic ozonation of high saline petrochemical wastewater using PAC@Fe^{II}Fe^{III}O₄: optimization, mechanisms and biodegradability studies, *Sep. Purif. Technol.*, 177 (2017) 293–303.
- [35] A. Ikhlaiq, D.R. Brown, B. Kasprzyk-Hordern, Catalytic ozonation for the removal of organic contaminants in water on alumina, *Appl. Catal., B*, 165 (2015) 408–418.
- [36] S.P. Tong, R. Shi, H. Zhang, C.A. Ma, Kinetics of Fe₃O₄-CoO/Al₂O₃ catalytic ozonation of the herbicide 2-(2,4-dichlorophenoxy) propionic acid, *J. Hazard. Mater.*, 185 (2011) 162–167.
- [37] J. Lee, S. Lee, S. Yu, D. Rhew, Relationships between water quality parameters in rivers and lakes: BOD₅, COD, NBOP₅, and TOC, *Environ. Monit. Assess.*, 188 (2016) 252.
- [38] G. Thompson, J. Swain, M. Kay, C.F. Forster, The treatment of pulp and paper mill effluent: a review, *Bioresour. Technol.*, 77 (2001) 275–286.
- [39] R. Rosal, M.S. Gonzalo, A. Rodríguez, J.A. Perdigón-Melón, E. García-Calvo, Catalytic ozonation of atrazine and linuron on MnO_x/Al₂O₃ and MnO_x/SBA-15 in a fixed bed reactor, *Chem. Eng. J.*, 165 (2010) 806–812.
- [40] S. Tong, R. Shi, H. Zhang, C. Ma, Catalytic performance of Fe₃O₄-CoO/Al₂O₃ catalyst in ozonation of 2-(2,4-dichlorophenoxy) propionic acid, nitrobenzene and oxalic acid in water, *J. Environ. Sci.*, 22 (2010) 1623–1628.
- [41] G. Abdelli, N.K.V. Leitner, Oxidation of cyanuric acid in aqueous solution by catalytic ozonation, *Ozone Sci. Eng.*, 38 (2015) 233–241.
- [42] A.A. Aghapour, G. Moussavi, K. Yaghmaei, Degradation and COD removal of catechol in wastewater using the catalytic ozonation process combined with the cyclic rotating-bed biological reactor, *J. Environ. Manage.*, 157 (2015) 262–266.
- [43] Y. Nie, N. Li, C. Hu, Enhanced inhibition of bromate formation in catalytic ozonation of organic pollutants over Fe-Al LDH/Al₂O₃, *Sep. Purif. Technol.*, 151 (2015) 256–261.
- [44] S. He, L. Pengcheng, M. Lihuan, X. Jun, L. Jun, Z. Liqi, Z. Jinsong, Mineralization of recalcitrant organic pollutants in pulp and paper mill wastewaters through ozonation catalyzed by Cu-Ce supported on Al₂O₃, *BioResources*, 13 (2018) 3686–3703.
- [45] F. Deng, S. Qiu, C. Chen, X. Ding, F. Ma, Heterogeneous catalytic ozonation of refinery wastewater over alumina-supported Mn and Cu oxides catalyst, *Ozone Sci. Eng.*, 37 (2015) 546–555.
- [46] C. Chen, B.A. Yoza, Y. Wang, P. Wang, Q.X. Li, S. Guo, G. Yan, Catalytic ozonation of petroleum refinery wastewater utilizing Mn-Fe-Cu/Al₂O₃ catalyst, *Environ. Sci. Pollut. Res.*, 22 (2015) 5552–5562.
- [47] Y. Wang, Y. Xie, H. Sun, J. Xiao, H. Cao, S. Wang, 2D/2D Nano-hybrids of γ -MnO₂ on reduced graphene oxide for catalytic ozonation and coupling peroxymonosulfate activation, *J. Hazard. Mater.*, 301 (2015) 56–64.
- [48] W.H. Shen, J. Li, X.Q. Chen, S.B. Wu, Z.F. Lin, X.H. Tian, Advanced treatment process for papermaking wastewater by composite photoelectrocatalysis and heterogeneous photocatalysis of nano-TiO₂ colloid and its pilot-scale system, *BioResources*, 14 (2019) 4454–4472.
- [49] J. Schmitt, H.-C. Flemming, FTIR-spectroscopy in microbial and material analysis, *Int. Biodeterior. Biodegrad.*, 41 (1998) 1–11.
- [50] W. Wattanathana, N. Nootsuwan, C. Veranitisagul, N. Koonsaeng, S. Suramitr, A. Laobuthee, Crystallographic, spectroscopic (FT-IR/FT-Raman) and computational (DFT/B3LYP) studies on 4,4'-diethyl-2,2'-[methylazanediylbis(methylene)]diphenol, *J. Mol. Struct.*, 1109 (2016) 201–208.
- [51] F.J. Chen, W.C. Yu, Y. Qie, L.X. Zhao, H. Zhang, L.H. Guo, Enhanced photocatalytic removal of hexavalent chromium through localized electrons in polydopamine-modified TiO₂ under visible irradiation, *Chem. Eng. J.*, 373 (2019) 58–67.
- [52] N. Srisasiwimon, S. Chuangchote, N. Laosiripojana, T. Sagawa, TiO₂/lignin-based carbon composited photocatalysts for enhanced photocatalytic conversion of lignin to high value chemicals, *ACS Sustainable Chem. Eng.*, 6 (2018) 13968–13976.
- [53] H. Zhang, S. Nie, C. Qin, K. Zhang, S. Wang, Effect of hot chlorine dioxide delignification on AOX in bagasse pulp wastewater, *Cellulose*, 25 (2018) 2037–2049.

- [54] N.B. Parilti, D. Akten, Optimization of $\text{TiO}_2/\text{Fe(III)}$ /solar UV conditions for the removal of organic contaminants in pulp mill effluents, *Desalination*, 265 (2011) 37–42.
- [55] I.J. Ani, U.G. Akpan, M.A. Olutoye, B.H. Hameed, Photocatalytic degradation of pollutants in petroleum refinery wastewater by TiO_2 and ZnO-based photocatalysts: recent development, *J. Cleaner Prod.*, 205 (2018) 930–954.
- [56] H. Park, J. Kim, H. Jung, J. Seo, H. Choi, Iron oxide nanoparticle-impregnated alumina for catalytic ozonation of par-chlorobenzoic acid in aqueous solution, *Water Air Soil Pollut.*, 225 (2014) 1–9.
- [57] D. Balabanic, M. Filipic, A. Krivograd Klemencic, B. Zegura, Raw and biologically treated paper mill wastewater effluents and the recipient surface waters: cytotoxic and genotoxic activity and the presence of endocrine disrupting compounds, *Sci. Total Environ.*, 574 (2017) 78–89.
- [58] J. Vittenet, W. Aboussaoud, J. Mendret, J.-S. Pic, H. Debellefontaine, N. Lesage, K. Faucher, M.-H. Manero, F. Thibault-Starzyk, H. Leclerc, Catalytic ozonation with $\gamma\text{-Al}_2\text{O}_3$ to enhance the degradation of refractory organics in water, *Appl. Catal., A*, 504 (2015) 519–532.
- [59] J. Yu, G. Wang, B. Cheng, M. Zhou, Effects of hydrothermal temperature and time on the photocatalytic activity and microstructures of bimodal mesoporous TiO_2 powders, *Appl. Catal., B*, 69 (2007) 171–180.
- [60] M. Kermani, B. Kakavandi, M. Farzadkia, A. Esrafil, S.F. Jokandan, A. Shahsavani, Catalytic ozonation of high concentrations of catechol over $\text{TiO}_2@\text{Fe}_3\text{O}_4$ magnetic core-shell nanocatalyst: optimization, toxicity and degradation pathway studies, *J. Cleaner Prod.*, 192 (2018) 597–607.